

# Independent Position Control of Two Magnetic Microrobots via Rotating Magnetic Field in Two Dimensions

Mohammad Salehizadeh\*, Zhaoxin Li\*, Eric Diller

**Abstract**—This paper introduces new strategy for motion control of two spinning magnetic agents based on the magnetic-fluidic interactions. The approach relies on balance between magnetic attraction and hydrodynamic repulsion forces created by fluidic vortices around pairs of microagents, which allows the control on inter-agent pair heading and spacing. The proposed method only requires a single global input, i.e., frequency of the rotating magnetic field along with a small magnetic field gradient, to control the motion of two microagents and therefore is simple to implement. Detailed finite element analysis is performed to explore the system behaviour. Finally, as experimental demonstration, two microagents are maneuvered by a global magnetic field to be independently positioned in the plane of motion with average root mean square errors of 140 micrometers and 5.68 degrees in separation and pair heading angle states, respectively.

**Keywords:** soft robotics, multi-agent underactuated control at microscales, magnetic-fluidic interactions, vortex, microrotors

## I. INTRODUCTION

Cooperative control of microagents plays an essential role in a variety of fields including microassembly, lab-on-a-chip systems, biological science, and minimally invasive surgical tool designs where access to small remote spaces is difficult.

There has been a lot of interest in researching the behaviours of microrobots in fluid. Using rotating magnetic field, the microrobots can behave like rotors in response to externally applied torques. Many manipulation tasks in confined workspace such as drug delivery, in-vivo injection, and tissue extraction can be achieved by manipulating microrotors. A variety of theoretical analyses and practical approaches of microrotors have been done in this field: Tottori et al. in [1] utilized rotating magnetic field to dynamically locomote, assemble, disassemble a cluster of magnetic chiral microstructures. Ongaro et al. in [2] designed a highly dexterous electromagnetic coil system by which they can independently control the position of two mobile magnetic microrobots in 3D using gradient action. Fily et al. [3] discussed two types of rotors and rotors' dynamics based on the flow field. Wang et al. [4] applied precessing magnetic field to control a group of self-assembled magnetic droplets for manipulation tasks. Buzhardt et al. [5] studied the controllability and path planning for two microrotors in Stokes flow. Yet, the ability to exert independent control over each agent in a team of microrobots working together on a task is highly needed to increase task dexterity.

This work is supported by the NSERC Discovery Grants Program.

M. Salehizadeh, Zhaoxin Li, and E. Diller are with the department of Mechanical and Industrial Engineering, University of Toronto, 5 King's College Road, Toronto M5S 3G8, Canada ediller@mie.utoronto.ca

\* M. Salehizadeh and Zhaoxin Li contributed equally to this work.

To achieve independent team control of magnetic microrobot agents for biomedical applications, an opportunity is to gain a deep understanding of magnetic-fluidic interactions between a pair of agents as the building block of team. Recently, a number of explorations have been made on swarm control of magnetic microrobots [6]–[10]. Nevertheless, none of them analyzed the magnetic-fluidic interactions specifically associated to a pair of agents in transverse direction of motion to the separation vector between pair of agents termed as pair heading.

Our previous work [11]–[15] introduced deterministic methods to control the motion of two or more spherical and functional agents in close proximity using homogeneous magnetic field by posing the system as an underactuated first-order kinematic problem. We hypothesize that using only a rotating magnetic field with modulated frequency one can achieve pair heading and spacing control for pair of agents in 2D. In this paper, we validate this hypothesis from fluid mechanics perspective. The concept is applied for two-agent configuration to simplify solving team of agents control. The goal is accomplished by modulating the magnetic-fluidic attraction or repulsion, clockwise or counter-clockwise rotations, and team center-of-mass (COM) pulling. In addition, the impact of different parameters such as frequency and viscosity on the motion are characterized and curve fitted into force equations.

The presented approach could be generalized to 3D, applied to a larger number of agents, and is workable no matter using identical or heterogeneous, hard or soft magnets, either having the coils set up far away or close, can be used to propel functional agents such as microrotors or helical microcarriers [16], and it is possible to be combined with other multi-agent control methods [4].

## II. CONCEPTS AND DEFINITIONS

This section studies the kinematics describing a pair of agents along with the spatiotemporal inter-agent magnetic-fluidic force relations, and lays the foundation for controlling a two-agent configuration.

Following the convention, magnetic flux density is denoted by  $\mathbf{B}$ . A magnetic moment  $\mathbf{m}$  represents the field orientation of a magnetic microrobot agent. We model each agent as a magnetic point dipole and so only consider the magnetic moment in force calculations. Under the act of an external magnetic field or via local magnetic interaction with other agents of a set, each agent may experience both force  $\mathbf{F}_m$  and torque  $\boldsymbol{\tau}$ , which can be calculated by  $\mathbf{F}_m = (\mathbf{m} \cdot \nabla)\mathbf{B}$  and

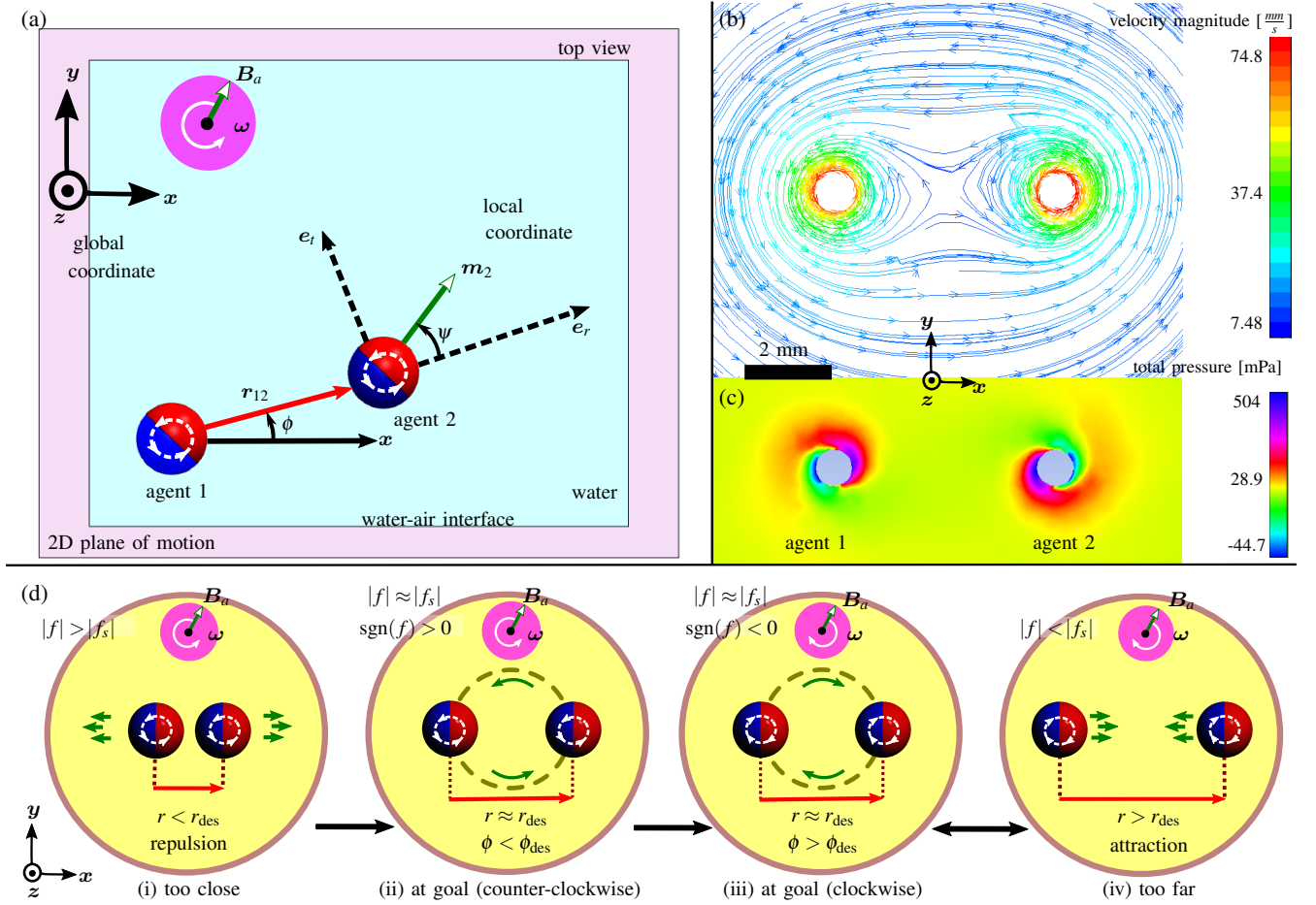


Fig. 1: The principles of the localized control of two microrobots on a horizontal 2D plane using rotating magnetic field (top view). Each agent rotates magnetically in place (depicted by white dashed circles) in response to an external rotating magnetic field  $B_a$ . The definitions of relevant parameters are given in (a) in both a global and a local coordinate frames. The two-agent separation vector pointing from agent 1 to 2 and the pair heading are denoted by  $r_{12}$  and  $\phi$ , respectively. The radial and transverse coordinates are shown by  $e_r$  and  $e_t$ . The control input is the frequency  $f$  at which the field rotates along the rotation axis  $\omega$  pointing normal to the horizontal plane. The net vortex fluid field around both agents are plotted in (b) and (c): top plot shows fluid velocity pathlines and bottom plot shows total pressure around two magnetic spinning spheres from top view. (d) States of microagent attraction or repulsion as well as pair heading rotation directions are determined by the frequency magnitude and its sign associated with the rotating global magnetic field  $B_a$ , respectively. The symbol  $\text{sgn}()$  represents the sign function.

$\tau = \mathbf{m} \times \mathbf{B}$ , where  $\nabla$  here is the Jacobian [17]. We base our analysis on the assumption that the magnetic moment  $\mathbf{m}$  of all magnetic agents in the workspace align with the applied field  $B_a$ . We use the frequency of the applied rotating field as our control input to the entire system.

#### A. Generation of Rotating magnetic field

Fig. 1 (a) shows two magnetic agents with the relevant kinematic parameterization floating at the liquid-air interface. The two agents rotate in place following the external rotating magnetic field  $B_a$  along the rotation axis  $\omega$  which is orthogonal to the horizontal plane of motion. In turn, vortex velocity field appears around each agent. The surface plots of the net vortex velocity and pressure fields at the 2D plane of motion are shown in Fig. 1 (b) and (c) obtained by ANSYS-FLUENT finite element analysis.

As the name implies, the inter-agent magnetic and fluidic forces are preferred to be studied in local Cylindrical coordinates ( $e_r, e_t, e_z$ ) where  $e_r$  lies along the separation

vector. The time average of magnetic inter-agent forces on agent 2 generated by rotating magnetic field over one revolution of the field is given by the following relations expressed in the proposed coordinate:

$$\langle F_{r_m} \rangle = -\frac{3\mu_0 m_1 m_2}{8\pi r_{12}^4} \hat{e}_r, \quad (1a)$$

$$\langle F_{t_m} \rangle = 0, \quad (1b)$$

$$\langle F_{z_m} \rangle = 0. \quad (1c)$$

Here  $\mu_0$  is the vacuum permeability,  $m_1$  and  $m_2$  are magnetic moments for agents 1 and 2, respectively. Time average operator is denoted by  $\langle \cdot \rangle$ .

#### B. Fluid mechanics of vortices

1) *Hydrodynamic forces*: Solving Navier-Stokes equation, the force acting on one agent by the generated fluid of another agent is obtained in [18] for low Reynolds number flow regime. Using finite element analysis, we developed

the following formula to ensure that it would meet two conditions: 1) the calculated radial and transverse forces are the ones that are acting on one agent by the superposed generated vortices created by the rotation of both agents. 2) the viscosity curve-fitted functions are also introduced into the hydrodynamic radial and transverse force relations as

$$\langle F_{r_h} \rangle = c_r \rho Q(\mu) \omega^2 \frac{R^7}{r^3} \hat{e}_r, \quad (2a)$$

$$\langle F_{t_h} \rangle = c_t \rho \mu \omega \frac{R^3}{r^2} \hat{e}_t, \quad (2b)$$

where the viscosity function in radial hydrodynamic force is estimated as

$$Q(\mu) = a\mu + b, \quad Re \leq 1 \quad (3)$$

Our finite element simulations provided in the next section implies that the viscosity function at laminar flow regime ( $Re \leq 1$ ) is linear. For  $f = 30\text{Hz}$  we found  $a = -0.17$  and  $b = 0.072$ . This paper only deals with Laminar flow regime and larger Reynolds number impact can be studied in future. It is remarkable that depending on viscosity, the radial force is not only repulsive but can also get attractive which will be discussed in the next section. In (2)  $c_r$  and  $c_t$  are the proportional constants,  $\rho$  is the fluid density,  $\mu$  is the fluid viscosity,  $\omega$  is the rotating angular speed, and  $R$  is the radius. The finite element simulations suggest that one can quantify the behaviour of system based on the viscosity and Reynolds number.

2) *step-out frequency*: A microagent modeled as a spherical robot rotates synchronously with the applied field at a given  $\omega$  as long as external magnetic torque balances the drag torque, exerted on each agent [19]. The step-out occurs when the drag torque beats the magnetic torque, in this case, the magnetization of robots lags the external field over  $90^\circ$ . Increasing the rotating frequency contributes to the increment of drag torque, resulting in step-out at:

$$\omega_{step-out} = \frac{BV_m M}{8\pi\mu R^3} \quad (4)$$

where  $B$  is the magnitude of the applied field,  $V_m$  is the volume, and  $M$  is the magnetization. By modeling the coil system as an RL circuit, the cut-off frequency was measured to be  $70\text{Hz}$  which is much smaller than the step-out frequency of the system.

### III. CONTROL OF TWO-AGENT CONFIGURATION

In this section, we discuss the properties and potentials that can be addressed based on finite element simulations and experiments. In sequel, we synthesize a control law to independently set the position of two agents to desired states in two dimensions.

#### A. Parameter Analysis

1) *Vortex build-up time*: There is a time interval  $\tau$  that allows fluid to build up from the initial hydrostatic state to the vortex steady state. In Fig. 2 (a) each point corresponds to an open-loop experiment performed at a given frequency. The

build-up time is obtained by observing the rise-time of speed or equivalently propelling force in the radial direction along the separation vector. The truncated transient state (shown in green) refers to the fact that by increasing frequency the net radial force, including both magnetic and hydrodynamic forces, changes from attractive to repulsive. The points during transient state can be ignored. The build-up time doesn't have large dependency on rotating frequency, and it ranges from 0.4s to 0.8s, which is within the reasonable range for controlling.

2) *Two-agent hydrodynamic frequency response*: At the viscosity of interest, the radial hydrodynamic force is expected to be repulsive and by increasing frequency the two agents will repel each other more strongly. Likewise, the transverse force increases with frequency and agents rotate faster in a certain direction. This property inspired us to consider frequency as our control input.

3) *Viscosity impact on motion*: We formulated the relation between viscosity and hydrodynamic forces using finite element simulations (see Fig. 2 (c) and (d)) and verified in experiment. As represented in (2) and (3), the force relation with viscosity at low Reynolds number range ( $\mu > 0.01$  or  $Re < 1$ ) can be approximated by a line. In addition, the radial force sign reversal happens by increasing the viscosity. This observation envisions that besides frequency another way to achieve control on separation state between a pair of agents is by changing the Reynolds number through viscosity. Another important observation is at lower viscosity the radial hydrodynamic force beats the transverse force, whereas at higher viscosity the transverse hydrodynamic force will dominate the radial one.

#### B. Controller design

The purpose of this part is to design a controller with frequency  $f$  as the only control input which makes the system underactuated. The basis for producing the associated radial and transverse forces is shown in Fig. 1 (d). As long as the rotation axis does not change from z-axis and agents float on a low viscosity liquid, the time average of magnetic inter-agent force stays always attractive, whereas the vortex-based radial hydrodynamic force is repulsive with a transverse force produced in a certain direction depending on the sign of frequency.

Here is our Bang-Bang control principle (see Fig. 1 (d)): When two agents are too close with respect to the desired separation ( $r < r_{des}$  note that  $r_{des}$  can change in experiment), the controller will repel them by increasing the frequency magnitude  $|f| > |f_s|$  where  $f_s$  is the setpoint, see (i). If two agents are too far, the controller will attract them by decreasing the frequency magnitude  $|f| < |f_s|$ , see (iv). Near the setpoint frequency of  $f_s$ , net radial force exerted on each agent becomes zero. By reversing the frequency sign, the rotation direction of the whole pair can be reversed, see (ii) and (iii).

To enhance the level of precision, a more sophisticated controller with intermediate frequencies centered around the zero-radial force frequency  $f_s$  would be chosen. That led us

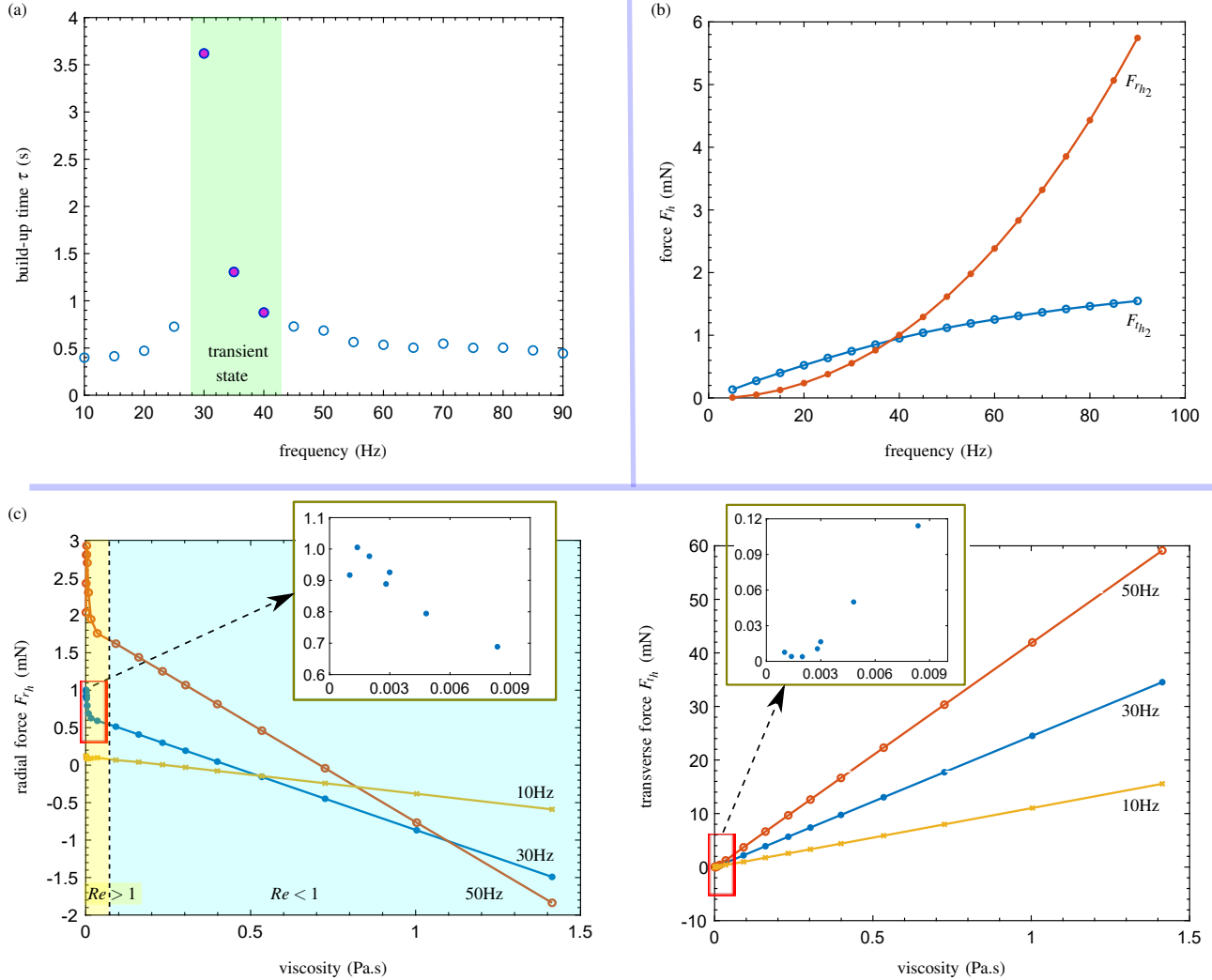


Fig. 2: (a) Build-up time for different rotating frequencies obtained from experiment. (b) Radial and transverse hydrodynamic forces on agent 2 as a function of rotating frequency from finite-element simulations (the liquid density and viscosity are  $\rho = 1.193 \times 10^3 \text{ kg/m}^3$  and  $\mu = 0.035 \text{ Pa}\cdot\text{s}$ ). (c) Radial and transverse hydrodynamic forces for different fluid viscosities from finite-element simulations. Forces on agent 1 were found to be similar with opposite sign within 2% from that of agent 2.

to the design of a proportional controller (P-controller) on separation state shown in Fig. 3 (a). We set the frequency upper and lower bounds  $f_U$  and  $f_L$  as 60Hz and 0Hz, respectively. Also we realized in experiment that there will be an angle delay appearing when switching the frequency sign to maintain pair heading angle at desired goal state, which results in a significant error. To solve this issue, we took benefit from a nonlinear controller on pair heading angle which can be described by a switching relay function illustrated in Fig. 3 (b). The pair heading state error and the deadzone half-width are denoted by  $\Delta\phi$  and  $\delta$ , respectively. The full description of the control algorithm is provided in Fig. 3 (c).

#### IV. RESULTS

This section introduces our fabrication method, experimental setup, and finally presents our experimental results.

##### A. Fabrication of agents and experimental setup

1) *Spherical agents*: Our spherical agents are composed of polyurethane polymer (BJB M-3184), which is mixed homogeneously with permanent magnetic particles (MQFP-15-7, NdPrFeB, Magnequench) at a mass ratio of 1:1, combined with hollow glass beads (3M<sup>TM</sup> Glass Bubbles K20) at a mass ratio of 10:1 to make the agents neutrally buoyant in order to float at the interface. These smooth spheres can be produced in a batch process using a fluid-assisted method as explained in [13]. We describe briefly this fabrication process involving: (1) Degas the prepared uncured composite in a vacuum pump. (2) Use a needle to inject this soft composite into a high viscous fluid such as 1000 cSt (25°C) silicon oil, honey, or corn syrup inside a beaker followed by a needle swirl. Afterwards, spheres are formed perfectly due to capillary force condensation. (3) Cure for 12 hours. (4) Clean the

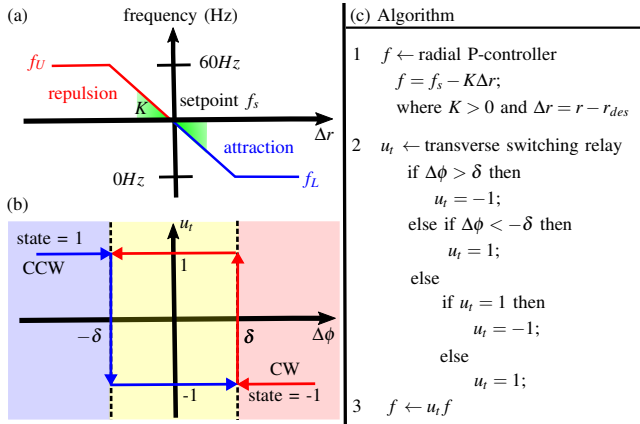


Fig. 3: (a) Radial proportional controller design for separation state. (b) Switching relay controller design for pair heading angle. The rotation direction of the applied rotating magnetic field is determined by frequency sign control input denoted by  $u_t$ . (c) Our control algorithm is rendered in pseudocode.

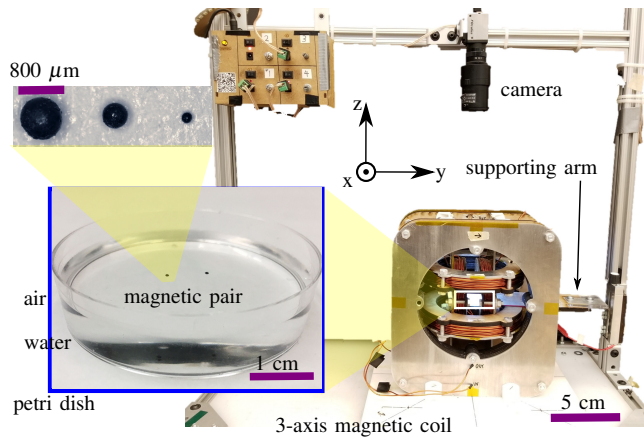


Fig. 4: Experimental setup. In the inset image of agent, two spherical microrobots sit at the interface of water-air inside a glass petri dish. The identical agents shown have a radius of  $400 \mu\text{m}$ . The agents are driven in horizontal plane by an electromagnetic coil system with three pairs of coils capable of producing fields in 3D.

spheres using water.

2) *Experimental setup*: Magnetic fields for agent actuation are created in an electromagnetic coil system with three pairs of coils nested orthogonally to create fields in 3D, powered by three pairs of analog servo drives (30A8, Advanced Motion Controls). Each pair of wire loops in the coil system is arranged in Helmholtz configuration, resulting in a uniform magnetic field up to 15 mT (uniform to within 5% of nominal at the center over a workspace size of 5 cm) located at center of the coil system (see Fig. 4). The strength of magnetic field is smaller than the coercivity of the magnetic materials in the agents, and so the agents magnetization will not be altered by the actuation field. Agent position is detected using a camera (FO134TC, FOculus) mounted atop the workspace, and a computer with custom Python code finds agent positions using a Hough Circle Transform in the OpenCV library at 60 frames/second. Two identical agents are immersed in a glass petri dish and

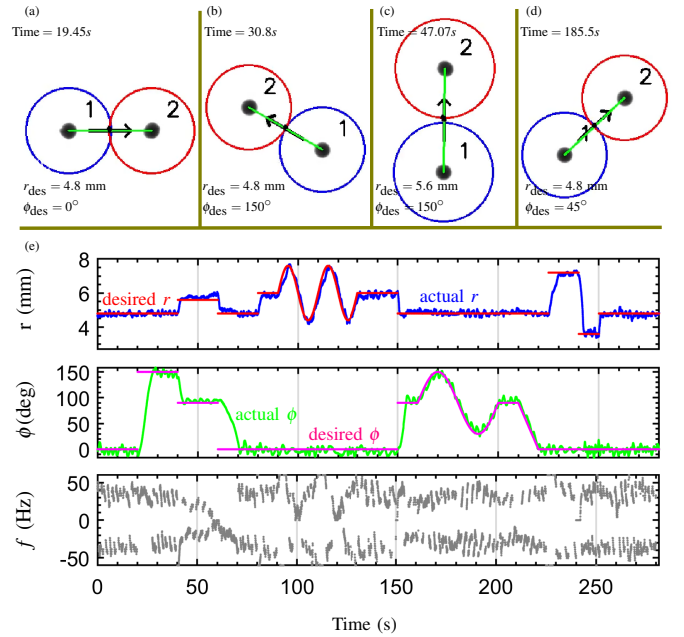


Fig. 5: (a)-(d) Candidate snapshots of the two-agent tracking experiment using the proposed frequency-based controller. The control task is to push agents toward desired separation and pair heading angle goals as noted at the bottom left of each image. The desired pairwise separation  $r_{\text{des}}$  is reached when the sketched surrounding colored circles around agents with radius equal to  $0.5r_{\text{des}}$  come into contact with one another. The desired pair heading angle  $\phi_{\text{des}}$  is reached when the green separation vector overlaps the sketched black arrow. The associated video is available as supplementary material. The red circle in the video represents the desired center-of-mass being tracked. (e) Separation  $r$  and pair heading angle  $\phi$  tracking and corresponding rotating frequency from experiment data.

sit at water-air interface as illustrated in Fig. 4.

## B. Experiment

We tested the proposed method on two-agent configuration to evaluate the performance of the controller. Fig. 5 shows the experimental result for the controller to track a changing goal state. RMS tracking error of less than 140 micrometers and 5.68 degrees is accomplished for the regulation of the separation  $r$  and the pair heading angle  $\phi$ , respectively. Thus, the frequency-based controller has the capability to operate as efficient as our previous controllers in [13]. Fig. 5 (a)-(d) presents four candidate snapshots associated to the given time. The control inputs are bounded and following a trend under the influence of the controller. Also one can control the center-of-mass (COM) position of the set of agents besides the relative states using a 2D magnetic field gradient that is superimposed on the uniform rotating field signal. Further details can be found at [13]. A video of this experiment is available in supplementary material.

## V. CONCLUSIONS

In this paper, we explored the 2D independent motion control of small-scale magnetic robots in close proximity with each other by changing frequency or viscosity under the act of a rotating magnetic field. Experimental results demonstrate that any inter-agent separation, heading, and

position of the set can be maintained via modulation of the inter-agent magnetic-fluidic forces.

For the controller to operate without instability, the relative spacing between agents in this work needed to be between 6 and 20 agents radius. Control over even smaller separations is limited because of three main reasons: 1) fluidic latency of vortices to build up, 2) the local field overpowers the external field for such small separation distances, 3) existing limit on feedback rate due to higher forces and fast system dynamics; hence, agents are susceptible to collision with each other. In this study, capillary interactions were assumed to be negligible. However, it is recommended to analyze these forces especially over extra small spacing.

Future research will investigate the problem of manipulating multiple agents to complete useful tasks using a team of agents in 3D fluidic environments and will implement complex motion tasks by changing the rotation axis additionally based on the general framework introduced in this work.

## REFERENCES

- [1] S. Tottori, L. Zhang, K. E. Peyer, and B. J. Nelson, "Assembly, disassembly, and anomalous propulsion of microscopic helices," *Nano letters*, vol. 13, no. 9, pp. 4263–4268, 2013.
- [2] F. Ongaro, S. Pane, S. Scheggi, and S. Misra, "Design of an electromagnetic setup for independent three-dimensional control of pairs of identical and nonidentical microrobots," *IEEE transactions on robotics*, 2018.
- [3] Y. Fily, A. Baskaran, and M. C. Marchetti, "Cooperative self-propulsion of active and passive rotors," *Soft Matter*, vol. 8, no. 10, pp. 3002–3009, 2012.
- [4] Q. Wang, L. Yang, B. Wang, E. Yu, J. Yu, and L. Zhang, "Collective behavior of reconfigurable magnetic droplets via dynamic self-assembly," *ACS applied materials & interfaces*, vol. 11, no. 1, pp. 1630–1637, 2018.
- [5] J. Buzhardt, V. Fedonyuk, and P. Tallapragada, "Pairwise controllability and motion primitives for micro-rotors in a bounded stokes flow," *International Journal of Intelligent Robotics and Applications*, vol. 2, no. 4, pp. 454–461, 2018.
- [6] B. Yigit, Y. Alapan, and M. Sitti, "Programmable collective behavior in dynamically self-assembled mobile microrobotic swarms," *Advanced Science*, p. 1801837, 2018.
- [7] J. Yu, B. Wang, X. Du, Q. Wang, and L. Zhang, "Ultra-extensible ribbon-like magnetic microswarm," *Nature communications*, vol. 9, no. 1, p. 3260, 2018.
- [8] E. Hunter, E. Steager, A. Hsu, A. Wong-Foy, R. Pelrine, and V. Kumar, "Nanoliter fluid handling for microbiology via levitated magnetic microrobots," *IEEE Robotics and Automation Letters*, 2019.
- [9] T. A. Howell, B. Osting, and J. J. Abbott, "Sorting rotating micromachines by variations in their magnetic properties," *Physical Review Applied*, vol. 9, no. 5, p. 054021, 2018.
- [10] A. W. Mahoney and J. J. Abbott, "Generating rotating magnetic fields with a single permanent magnet for propulsion of untethered magnetic devices in a lumen," *IEEE Transactions on Robotics*, vol. 30, no. 2, pp. 411–420, 2014.
- [11] M. Salehizadeh and E. Diller, "Two-agent formation control of magnetic microrobots," in *Int. Conf. Manipulation, Automation and Robotics at Small Scales*, 2016, pp. 1–6.
- [12] K. Choi, M. Salehizadeh, R. B. Da Silva, N. Hakimi, E. Diller, and D. K. Hwang, "3d shape evolution of microparticles and 3d enabled applications using non-uniform uv flow lithography (nufli)," *Soft matter*, vol. 13, no. 40, pp. 7255–7263, 2017.
- [13] M. Salehizadeh and E. Diller, "Two-agent formation control of magnetic microrobots in two dimensions," *Journal of Micro-Bio Robotics*, vol. 12, no. 1-4, pp. 9–19, 2017.
- [14] J. Zhang, M. Salehizadeh, and E. Diller, "Parallel pick and place using two independent untethered mobile magnetic microgrippers," in *IEEE Int. Conf. Robot. Autom.*, 2018, pp. 1–6.
- [15] M. Salehizadeh and E. Diller, "Optimization-based formation control of underactuated magnetic microrobots via inter-agent forces," in *Int. Conf. Manipulation, Automation and Robotics at Small Scales*, 2017, pp. 1–5.
- [16] H.-W. Huang, T.-Y. Huang, M. Charilaou, S. Lyttle, Q. Zhang, S. Pané, and B. J. Nelson, "Investigation of magnetotaxis of reconfigurable micro-origami swimmers with competitive and cooperative anisotropy," *Advanced Functional Materials*, vol. 28, no. 36, p. 1802110, 2018.
- [17] M. P. Kummer, J. J. Abbott, B. E. Kratochvil, R. Borer, A. Sengul, and B. J. Nelson, "Octomag: An electromagnetic system for 5-dof wireless micromanipulation," *IEEE Transactions on Robotics*, vol. 26, no. 6, pp. 1006–1017, 2010.
- [18] B. A. Grzybowski, X. Jiang, H. A. Stone, and G. M. Whitesides, "Dynamic, self-assembled aggregates of magnetized, millimeter-sized objects rotating at the liquid-air interface: macroscopic, two-dimensional classical artificial atoms and molecules," *Physical Review E*, vol. 64, no. 1, p. 11603, 2001.
- [19] E. Diller, Z. Ye, and M. Sitti, "Rotating magnetic micro-robots for versatile non-contact fluidic manipulation of micro-objects," in *Intelligent Robots and Systems (IROS), 2011 IEEE/RSJ International Conference on*. IEEE, 2011, pp. 1291–1296.